Computer and Telecommunication Engineering 2025, 3(1), 2911
https://doi.org/10.54517/cte2911

Brief Report

Spectral analysis of the Lorenz attractor

H. Ali Pacha[1,*], W. Aggoune[2], S. Hamaci[1], P. Lorenz[3], A. Ali Pacha[4]

[1] Quartz Laboratory, École Catholique d'Arts et Métiers-École d'Électricité, de Production et des Méthodes Industrielles (ECAM-EPMI), 95092 Cergy Pontoise, France
[2] Quartz Laboratory, École Nationale Supérieure de l'Électronique et de ses Applications (ENSEA), 95014 Cergy-Pontoise, France
[3] IRIMAS Institute, University of Haute Alsace, 68008 Mulhouse, France
[4] LACOSI Laboratory, University of Sciences and Technologies Oran, Oran 31000, Algeria
*** Corresponding author:** H. Ali Pacha, h.ali-pacha@ecam-epmi.com

CITATION

Ali Pacha H, Aggoune W, Hamaci S, et al. Spectral analysis of the Lorenz attractor. Computer and Telecommunication Engineering. 2025; 3(1): 2911. https://doi.org/10.54517/cte2911

ARTICLE INFO

Received: 30 August 2024
Accepted: 15 October 2024
Available online: 27 February 2025

Abstract: For a long time, chaos was considered uncontrollable and unusable. However, over the past thirty years, researchers have formulated equations for certain chaotic phenomena, revealing a deterministic aspect to what initially seems random. The evolution of chaotic systems is characterized by strange attractors, which, despite their complex nature, do not allow precise long-term predictions of system behavior. The Lorenz attractor is the best-known example and was the first to be studied, though many other attractors with unusual shapes have since been discovered. The aim of this work is to perform a spectral analysis of the Lorenz attractor by examining the frequencies present in the time signals generated by the solutions of the Lorenz system of equations. To evaluate the frequency complexity of these signals, the discrete Fast Fourier Transform (FFT) is used to derive their frequency spectrum.

Keywords: fast Fourier transform; spectral analysis; strange attractor; Lorenz attractor
Subject Classification (2010): 34A45; 34H10; 37M05; 65L03; 65L06; 68P25; 94A60

1. Introduction

For several years researchers have been interested in the possibility of using chaotic signals in data transmission systems to transmit large amounts of secure information [1]. The value of using chaotic signals lies in two core properties of chaos.

A chaotic signal is a signal with a wide spectrum, making it possible to transmit very varied signals. Moreover, a chaotic signal is obtained from a deterministic system, it is, therefore, possible to reconstitute it by placing oneself in the same conditions that contributed to its creation, thereby recovering the initial information. In 1963, Lorenz established a very simplified atmospheric model that has a strong sensitivity to initial conditions. This property explains the chaotic behavior of the model's solutions. This famous attractor is the most studied to date [2].

To better exploit these chaotic systems, it is important to understand their frequent behavior (this by performing a spectral analysis of their signals), because we already have a good understanding of their temporal behavior. This is to allow us to exploit their potential to the maximum.

The objective of this work is to perform a spectral analysis of the Lorenz attractor, focusing on identifying the dominant frequencies and spectral features of the chaotic system described by the Lorenz equations. The goal is to isolate the deterministic components of the attractor's coordinates from the chaotic ones, retaining only the chaotic elements for applications in data confidentiality [1].

2. Lorenz attractor

The Lorenz attractor is a fractal structure that emerges in the dynamical system described by the Lorenz differential equations, introduced by Edward Lorenz in 1963, exhibiting chaotic behavior under certain parameter values [3–6], resulting in completely unpredictable dynamics that never repeat. This phenomenon is known as sensitivity to initial conditions, which is a defining characteristic of chaotic systems. The Lorenz system equations are:

$$\begin{cases} \dfrac{dx}{dt} = s.(y - x) \\ \dfrac{dy}{dt} = r.x - y - x.z \\ \dfrac{dz}{dt} = x.y - b.z \end{cases} \quad (1)$$

s, r and b are positive reals parameters of the system. For specific values of these parameters, the system exhibits chaotic behavior, creating the Lorenz attractor, a double spiral **Figure 1**.

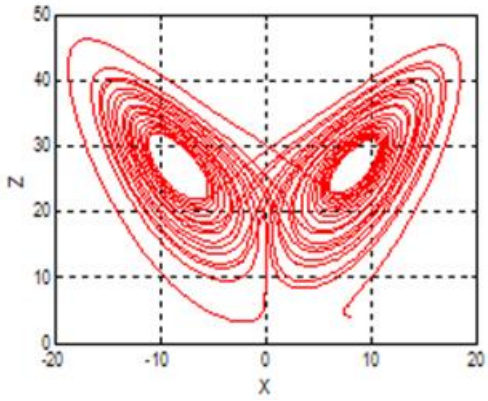

Figure 1. View of the Lorenz attractor in 3D.

It is important to note that this is a non-linear equation due to the x*z and x*y. This system of equations is generally non-integrable. This system must be solved using an approximation method (Euler Runge-Kutta) on a computer, once the three parameters *s*, *b*, and *r* have been set. We used the Runge-Kutta method. There are several variations of this method (order 3, 4, 5, ...). We will focus on the fourth-order Runge-Kutta method [7], which calculates the function's value at four intermediate points.

Due to the large number of calculations required (approximately 100,000), we will use a program written in Python. This program outputs the values of the three sequences into a file, based on the initial conditions and predefined variables. The visualization of the plots is done using the same language.

Our software is implemented in an advanced programming language [8], recently, designed by the firm Python Software Foundation—Python version 3.11.4. PYTHON consists of a relatively small core, capable of interpreting and then evaluating the matrix numeric expressions addressed to it.

The time signals associated with the coordinates *X(t)*, *Y(t)*, and *Z(t)* in the Lorenz system are crucial for understanding its chaotic dynamics. These signals, which are

functions of time, describe the evolution of the three variables over time and reveal how the coordinates oscillate in a complex and nonlinear manner.

The plots in the figures below were obtained with s = 10; r =28; b = 8/3 and a pitch (h) of 0.005. With the following initial conditions xo = 8; yo = 3; zo = 4. The evolution over time of such a system is chaotic. This can be "noted" intuitively thanks to the curves (**Figure 2** of the coordinate *X(t)*, **Figure 3** of the coordinate *Y(t)* and **Figure 4** of the coordinate *Z(t)*) [4] in a window of [0: 40]:

2.1. Behavior of the time signals

The differential equations of the Lorenz system generate irregular oscillations for each coordinate *X(t)*, *Y(t)*, and *Z(t)*. These time-signals show the values of these variables at every instant t, and all three are interdependent.

2.1.1. Coordinate *X(t)*

The time signal *X(t)* oscillates between positive and negative values, representing chaotic transitions between two regions in the Lorenz attractor. The variations in *X(t)* reflect the shifts from one lobe of the attractor to the other.

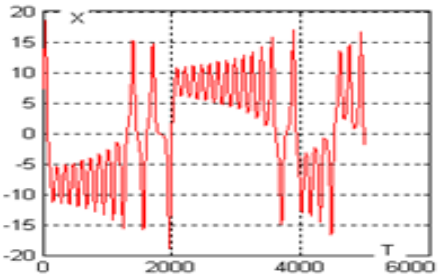

Figure 2. Lorenz attractor x-curve.

- Signal shape: The signal *X(t)* is irregular, with periods of rapid fluctuation and other periods of slower variation. There are sudden peaks followed by abrupt changes in direction.
- Amplitude: The magnitude of *X(t)* varies around two main regions (corresponding to the two lobes of the attractor), with values ranging from near zero to large amplitudes.

2.1.2. Coordinate *Y(t)*

The signal *Y(t)* is also chaotic, with similar variations to *X(t)*, but it represents a different component of the motion in phase space. The behavior of *Y(t)* is also influenced by the dynamics of both *X(t)* and *Z(t)*, making it a highly nonlinear signal.

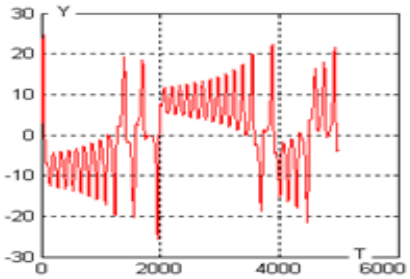

Figure 3. Lorenz attractor y-curve.

- Phase with *X(t)*: *Y(t)* and *X(t)* are generally correlated in time, but with a phase shift. They may appear to oscillate in sync for a period, then desynchronize unpredictably.
- Chaotic behavior: Like *X(t)*, the oscillations of *Y(t)* do not follow regular patterns. Each oscillation is unique and depends on previous values.

2.1.3. Coordinate *Z(t)*

The signal *Z(t)* differs from the others because it represents altitude (or "temperature" in the physical interpretation of the Lorenz model). It remains strictly positive and its variations, while more regular than *X(t)* and *Y(t)*, are still chaotic.

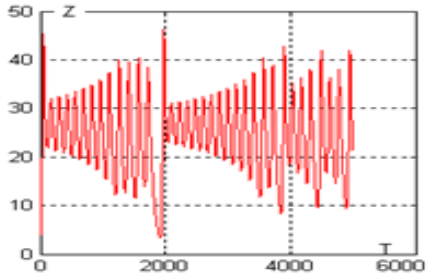

Figure 4. Lorenz attractor z-curve.

- Positive values: Unlike *X(t)* and *Y(t)*, *Z(t)* always stays above zero, although it can fluctuate over a wide range of values.
- Slow and fast variations: At certain times, *Z(t)* evolves slowly over extended periods, followed by rapid jumps, linked to chaotic transitions in the system.

2.2. Temporal properties of chaotic signals

- Non-periodic Oscillations: The time signals *X(t)*, *Y(t)*, and *Z(t)* are aperiodic. They never return exactly to a previous state, and it is impossible to predict when a certain behavior will repeat, even approximately.
- Quasi-repetitive behavior: Although there is no strict periodicity, the signals sometimes display behaviors that resemble repetition. For instance, a sequence of values in *X(t)* may resemble a previous one, but it will never be the same.

The time signals of the coordinates *X(t)*, *Y(t)*, and *Z(t)* in the Lorenz attractor exhibit irregular oscillations with no periodicity, but they maintain complex intercorrelations. Their seemingly random appearance directly reflects the chaotic nature of this system, where small initial differences can lead to drastically different outcomes. Analyzing these signals reveals the richness and complexity of deterministic chaos within the Lorenz model.

3. Spectral analysis

The spectral analysis of the Lorenz attractor involves examining the frequencies present in the time signal derived from the solution of the Lorenz equations.

3.1. Fourier transform

A common method for analyzing the spectrum of a signal is the Fourier transform, which enables the transition from the time domain to the frequency domain. By applying a Fourier transforms to the solutions *x(t)*, *y(t)*, and *z(t)*, the corresponding

power spectrum is obtained.

The first notion that we have of a signal is simply that of the measurement over time of any physical quantity, this quantity is often electrical, but it can also be optical, acoustic, and thermal. In nature almost all signals exist in analogy form, however in some devices, the processed signals are only defined by discrete time values: We then speak of time, discrete time, or sampled signal.

The Fourier transformation of a signal *x(nt)* sampled at the rate t is called discrete Fourier transformation (TDF) the result of this operation is a finite sequence of numbers.

The Fourier transformation of a signal *x(nt)*, sampled at the rate t, is referred to as the discrete Fourier transformation (DFT). The result of this operation is a finite sequence of numbers.

3.2. Fast Fourier transform

The Fast Fourier Transform (FFT) is an efficient algorithm for computing the Discrete Fourier Transform (DFT) and its inverse. The DFT converts a discrete signal from the time domain into the frequency domain by decomposing the signal into a sum of sinusoids at different frequencies.

Cooley and Tukey [9–11] proposed a method that considerably reduces the computation time of the discrete Fourier transform DFT of a sequence whose number of samples N is large and factor-decomposable (preferably when N is a power of 2). As a result, many often equivalent algorithms have been published; they are known by the general term FFT (Fast Fourier Transform).

All these algorithms are based on the same principle which consists in decomposing the calculation of the DFT of a sequence of length N into several DFTs of smaller length in order to exploit the symmetry and the periodicity of the complex exponential. The implementation of this principle leads to different methods whose performances are comparable. One distinguishes the two traditional types of algorithms interlacing in time and interlacing frequency in the case or $N = 2^L$. In time interleaving, the number of calculations is the same as in frequency interleaving; the transformed numbers *X(k)* appear in natural order while the numbers to be transformed *X(n)* are permuted.

In fact, to each time interleaving algorithm corresponds a frequency interleaving algorithm, obtained by allowing entry and exit and reversing the direction of the arrows in the graph. Let $\{x_n\}$ be the DFT of a sequence $\{x_k\}$ of length $N = 2^L$:

$$X(n) = \sum_{k=0}^{N-1} x_0(k) \,.\, e^{\frac{-j2\pi kn}{N}}; n = 0, 1, \dots, N-1 \quad (2)$$

where $N = 2^L$ is the number of signal samples.

The FFT reduces the computational complexity of the DFT from $O(N^2)$ to O (N Log N), making it significantly faster for large data sets. This efficiency is crucial in applications like audio processing, image compression, and solving partial differential equations.

4. Results interpretations

We implemented the FFT and the IFFT in our software after the prior realization of the components of the LORENZ attractor. The results of these components are as follows:

4.1. Direct fast Fourier transform of the Lorenz attractor

We will analyze the three graphs (**Figures 5–7**), obtained via the direct fast Fourier transform, by zooming in on each of these figures in three parts, as follows:

- The part going from 1 to 256: Graph on the left, noted (a).
- The part going from 256 to 3840: Graph in the Middle, noted (b).
- The part going from 3840 to 4096: Graph on the Right, noted (c).

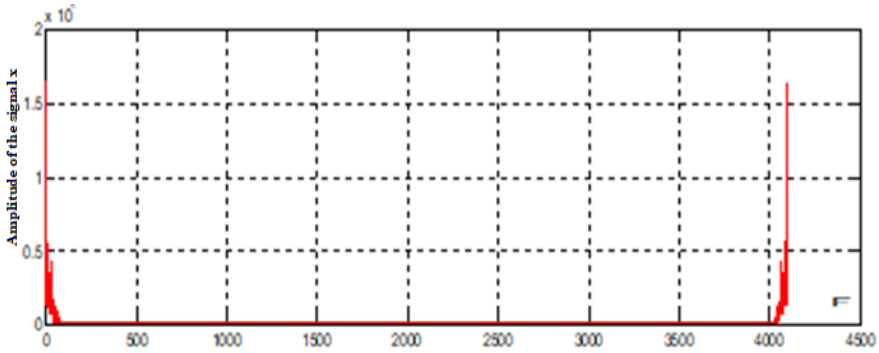

Figure 5. Fast Fourier transform of (dx/dt).

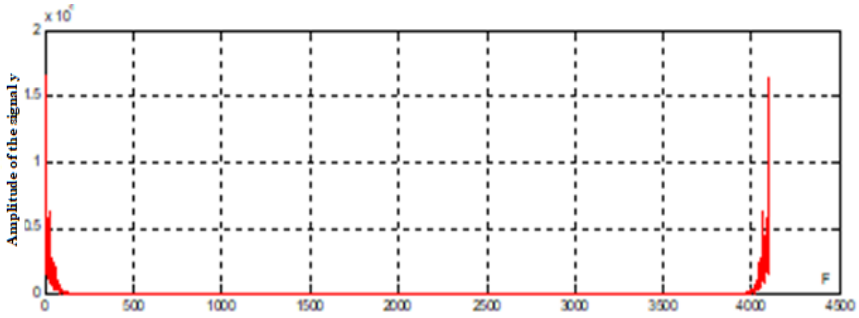

Figure 6. Fast Fourier transform of (dy/dt).

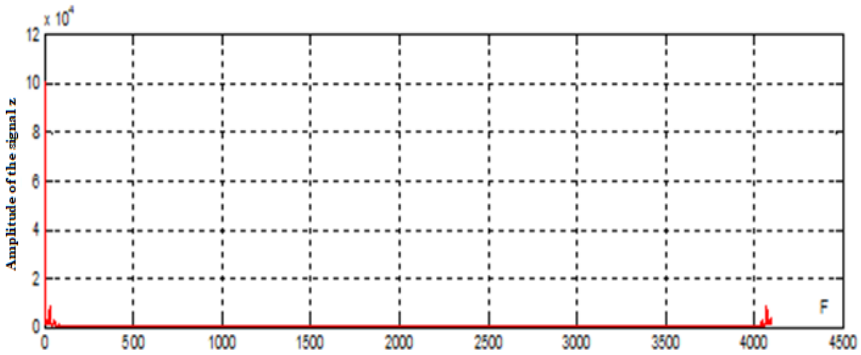

Figure 7. Fast Fourier transform of (dz/dt).

4.1.1. Fast Fourier transform of the dx/dt component of the Lorenz attractor

It should be noted that the graph in **Figure 5**, obtained by the direct fast Fourier transform, has the following form and is zoomed into three parts represented in **Figure 8**:

1) In the interval [1: 256], the resulting curve reaches a maximum value of 16,500 and displays an irregular or non-periodic pattern.
2) In the interval [256: 3840] we obtained the following curve this curve has a maximum value equal 28.5. It takes the shape of a tank, identified with X^2.
3) In the interval [3840: 4096] the resulting curve reaches a maximum value of 16,500 and displays an irregular or non-periodic pattern.

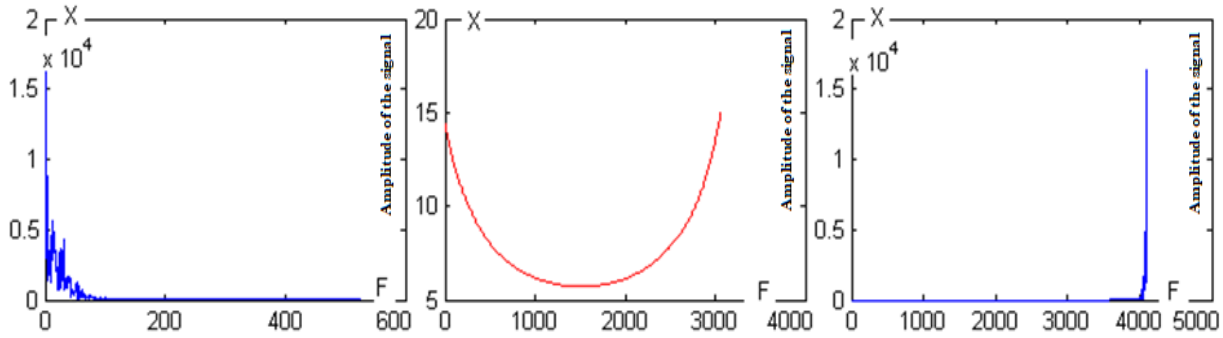

Figure 8. The curve represents the fast Fourier transform (FFT) of dx/dt divided into three regions for spectral analysis. **(a)** [1: 256] interval; **(b)** [256: 3840] interval; **(c)** [3840: 4096] interval.

4.1.2. Fast Fourier transform of the dy/dt component of the Lorenz attractor

It should be noted that the graph in **Figure 6**, obtained by the direct fast Fourier transform, has the following form and is zoomed into three parts represented in **Figure 9**:

1) In the interval [1: 256], the resulting curve has a maximum value of 16,624 and displays an irregular or non-periodic pattern.
2) In the interval [256: 3840] we obtained the following curve this curve has a maximum value equal 19.21. It takes the shape of a tank, identified with X^2.
3) In the interval [3840: 4096] we have obtained the following curve: this curve has a maximum value of 16,600 and has an irregular or non-periodic pattern.

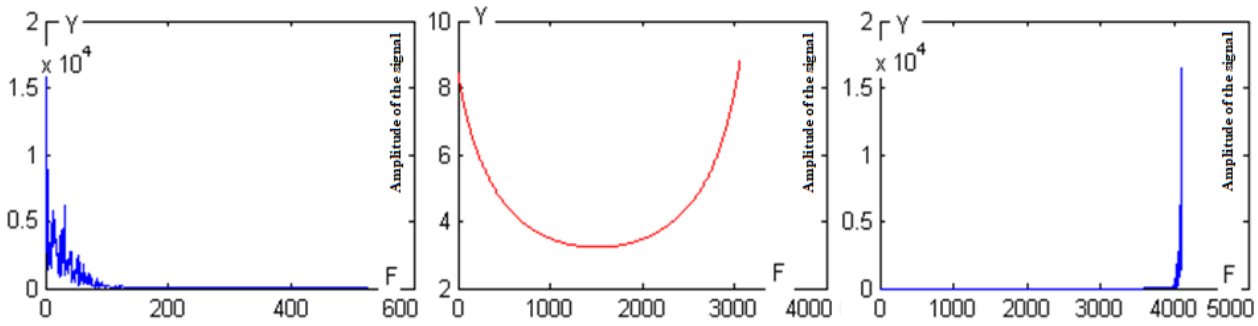

Figure 9. The curve represents the fast Fourier transform (FFT) of dy/dt divided into three regions for spectral analysis. **(a)** [1: 256] interval; **(b)** [256: 3840] interval; **(c)** [3840: 4096] interval

4.1.3. Fast Fourier transform of the dz/dt component of the Lorenz attractor

It should be noted that the graph in **Figure 7**, obtained by the direct fast Fourier transform, has the following form and is zoomed into three parts represented in **Figure 10**:

1) In the interval [1: 256], the resulting curve has a maximum value of 10,000 and exhibits an irregular or non-periodic pattern.
2) In the interval [256: 3840] we obtained the following curve this curve has a maximum value equal to 40.32. It takes the shape of a tank, identified with X^2.
3) In the interval [3840: 4096] we have obtained the following curve: this curve has a maximum value equal to 8660 and has an irregular or non-periodic pattern.

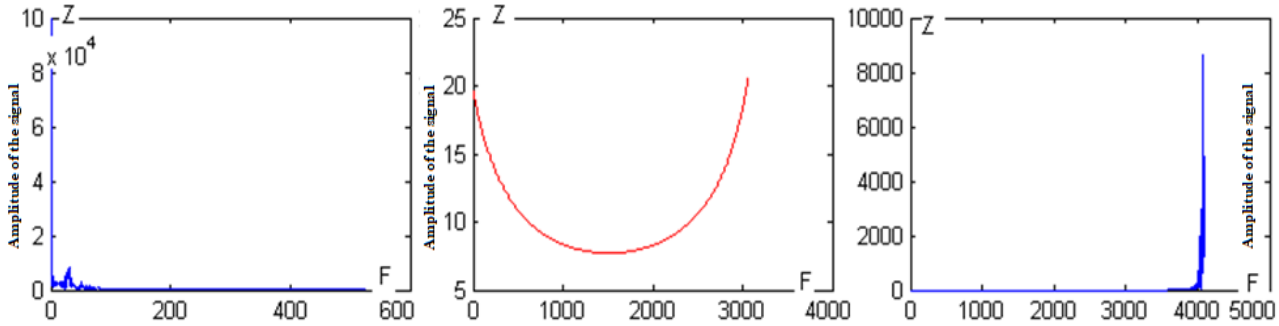

Figure 10. The curve represents the fast Fourier transform (FFT) of dz/dt divided into three regions for spectral analysis. **(a)** [1: 256] interval; **(b)** [256: 3840] interval; **(c)** [3840: 4096] interval

4.2. Inverse fast Fourier transform of the Lorenz attractor

We will analyze the three graphs (**Figures 11–13**), obtained via the direct inverse Fourier transform, by zooming in on each of these figures in three parts, as follows:

- The part going from 1 to 256: Graph on the left, noted (a).
- The part going from 256 to 3840: Graph in the Middle, noted (b).
- The part going from 3840 to 4096: Graph on the Right, noted (c).

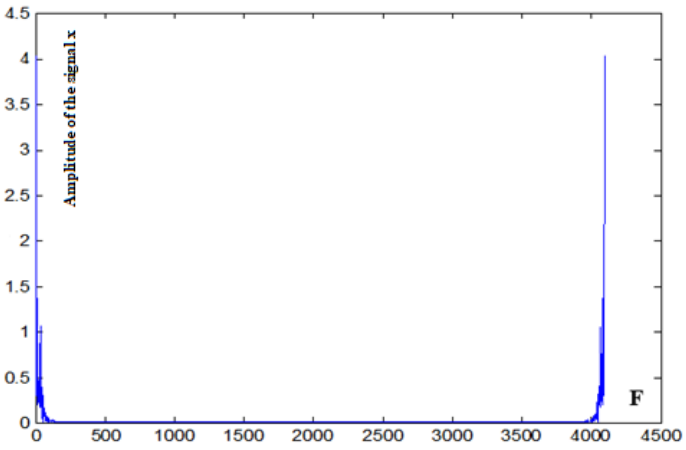

Figure 11. Fast Fourier transform inverse of (dx/dt).

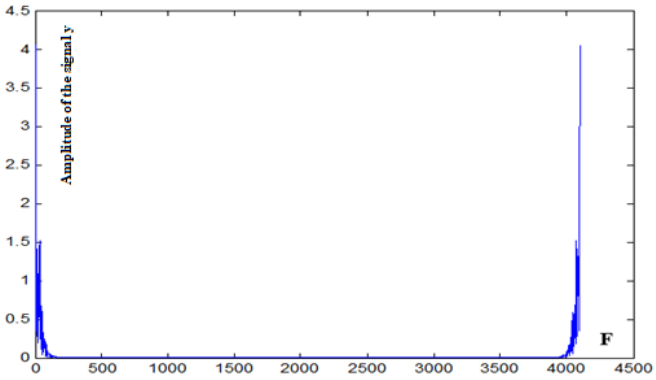

Figure 12. Fast Fourier transform inverse of (dy/dt).

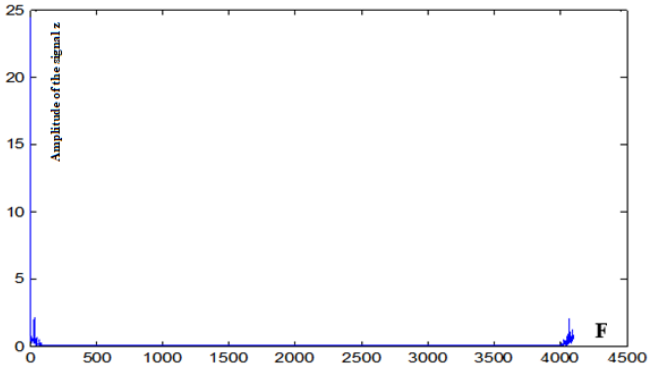

Figure 13. Fast Fourier transform inverse of (dz/dt).

4.2.1. Fast Fourier transform inverse of the dx/dt component of the Lorenz attractor

It should be noted that the graph in **Figure 11**, obtained by the inverse fast Fourier transform, has the following form and is zoomed into three parts represented in **Figure 14**:

1) In the interval [1: 256], the resulting curve has a maximum value of 4.02 and exhibits an irregular or non-periodic pattern.
2) In the interval [256: 3840] we obtained the following curve this curve has a maximum value equal 0.007
3) In the interval [3840: 4096] we obtained the following curve this curve has a maximum value equal 4.02 and has an irregular or non-periodic pattern.

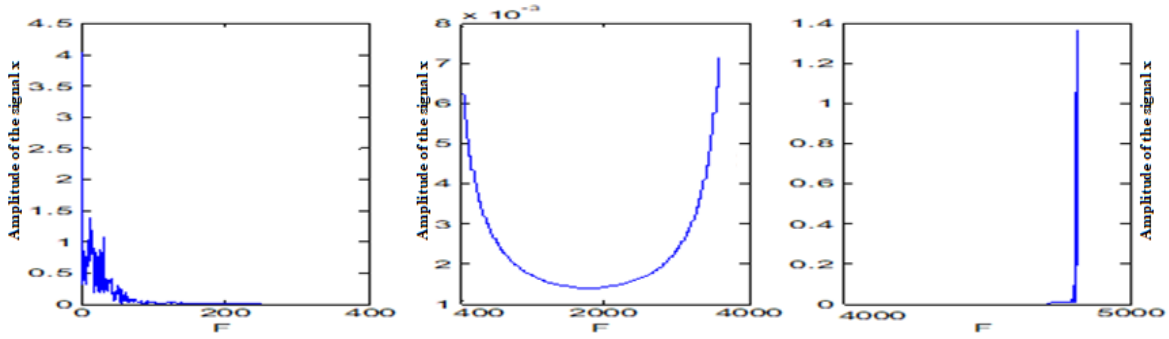

Figure 14. The curve represents the fast Fourier transform inverse (FFT) of dx/dt divided into three regions for spectral analysis. **(a)** [1: 256] interval; **(b)** [256: 3840] interval; **(c)** [3840: 4096] interval

4.2.2. Fast Fourier transform inverse of the dy/dt component of the Lorenz attractor

It should be noted that the graph in **Figure 12**, obtained by the inverse fast Fourier transform, has the following form and is zoomed into three parts represented in **Figure 15**:

1) In the interval [1: 256] we obtained the following curve this curve has a maximum value equal to 4.06 and has an irregular or non-periodic pattern.
2) In the interval [256: 3840] we obtained the following curve this curve has a maximum value equal to 0.0046
3) In the interval [3840: 4096] we obtained the following curve this curve has a maximum value equal to 4.06 and has an irregular or non-periodic pattern.

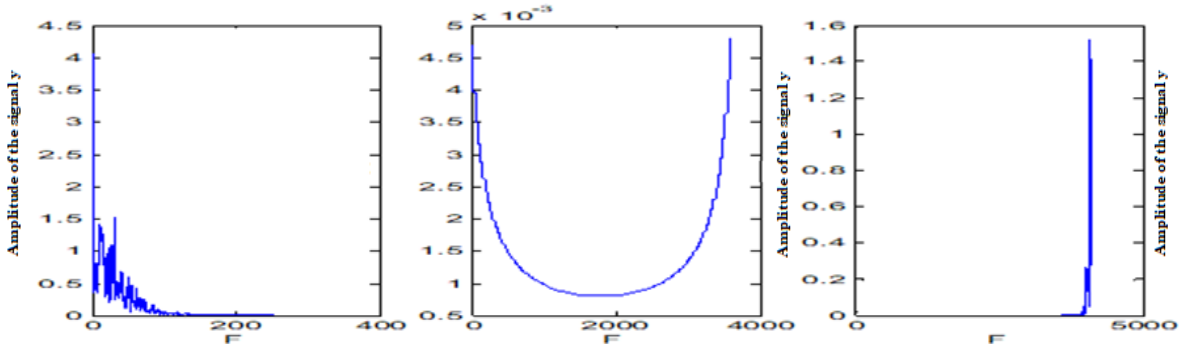

Figure 15. The curve represents the fast Fourier transform inverse (FFT) of dy/dt divided into three regions for spectral analysis. **(a)** [1: 256] interval; **(b)** [256: 3840] interval; **(c)** [3840: 4096] interval

4.2.3. Fast Fourier transform inverse of the dz/dt component of the Lorenz attractor

It should be noted that the graph in **Figure 13**, obtained by the inverse fast Fourier transform, has the following form and is zoomed into three parts represented in **Figure 16**:

1) In the interval [1: 256] we obtained the following curve this curve has a maximum value equal to 24.418 and has an irregular or non-periodic pattern.
2) In the interval [256: 3840] we obtained the following curve this curve has a maximum value equal 0.0098.
3) In the interval [3840: 4096] we obtained the following curve this curve has a maximum value equal to 2.1137 and has an irregular or non-periodic pattern.

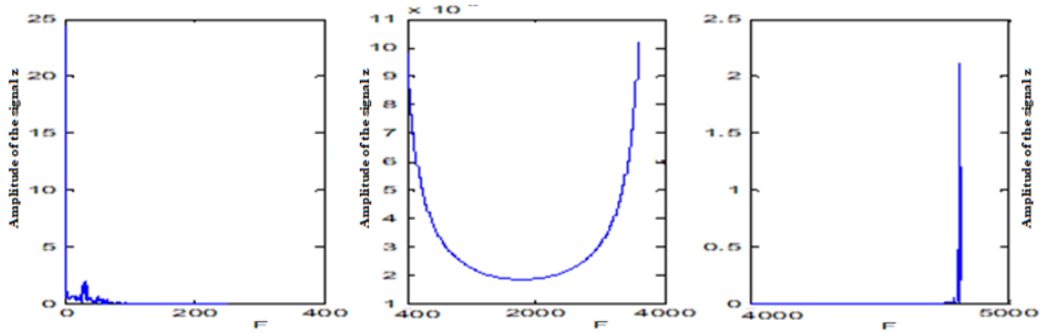

Figure 16. The curve represents the fast Fourier transform inverse (FFT) of dz/dt divided into three regions for spectral analysis. **a)** [1: 256] interval; **(b)** [256: 3840] interval; **(c)** [3840: 4096] interval

4.3. Result to remember

From the slices of the curves obtained by the direct fast Fourier transform of the signals (dx/dt) in **Figure 17**, (dy/dt) in **Figure 18** and (dz/dt) in **Figure 19**, we apply the inverse fast Fourier transform to each slice of these "significant" curves and we visualize the results of these signals in three dimensions.

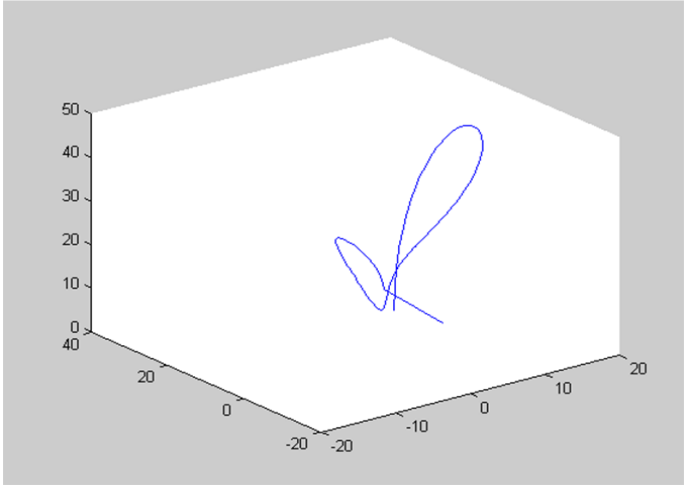

Figure 17. FFT(IFFT) which corresponds to the [1: 256] interval.

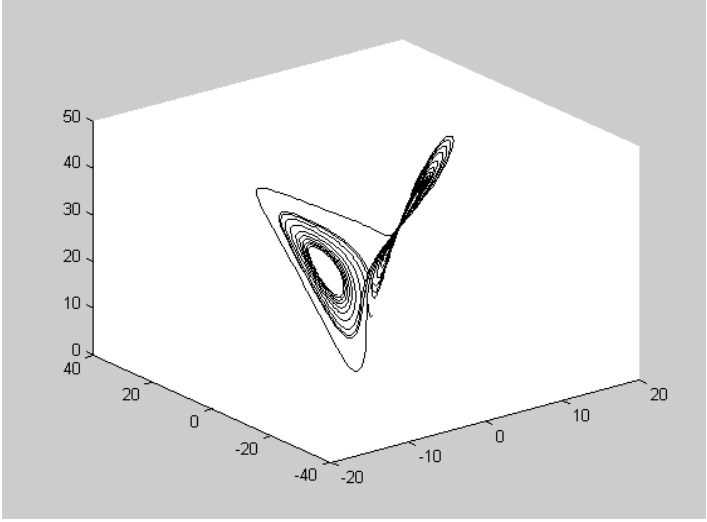

Figure 18. FFT(IFFT) which corresponds to the [256, 3840] interval.

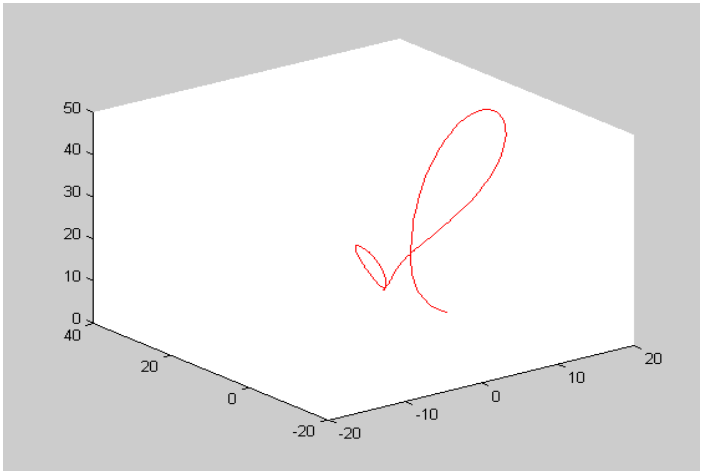

Figure 19. FFT(IFFT) which corresponds to the [3840, 4096] interval.

1) Curve 14 is obtained in the interval [1: 256]:
2) In the interval [256: 3840], we obtain the following curve 15:
3) Then, we take the interval [3840: 4096] and the curve that presents itself is 16.

We have noticed that the Lorenz attractor exists in the interval [256: 3840]. In this interval, the dx/dt, dy/dt and dz/dt components all exhibit a tank shape identifiable with X^2.

5. Conclusion

The primary objective of our work was to analyze the properties of chaotic signals derived from the Lorenz differential equations. We applied both the direct and inverse FFT to better understand the system's behavior in the frequency domain. The results revealed that the FFT spectrum of the Lorenz attractor exhibits a pseudo-symmetric structure.

One of our key findings was that the Lorenz attractor can be effectively represented within the frequency range [256, 3840], and that the time derivatives (dx/dt, dy/dt, dz/dt) exhibit a parabolic form beyond this range. This suggests that most of the attractor's dynamic behavior is captured within this interval, while the frequencies outside of it show a more regular, parabolic trend. However, we were unable to precisely characterize this parabolic shape with a specific mathematical function.

This challenge may stem from two primary factors:

1) Complex Non-linearities: The parabolic shape observed could be due to intricate non-linearities within the Lorenz equations, making it difficult to model using simple quadratic or classical analytical forms. More complex functions or combinations of functions may be required to effectively capture these non-linearities.
2) Transcendental Behaviors: If the parabolic shape cannot be described by a classical polynomial function, it may indicate an underlying transcendental relationship. This could involve modified exponential, logarithmic, or trigonometric functions. Fitting these types of functions could provide a more accurate representation of the observed dynamics.
3) Future Directions:

- Interpolation and Data Resolution: A detailed examination of interpolation within the [256, 3840] frequency range is essential to accurately characterize the Lorenz attractor. Addressing data gaps and improving the resolution will provide a more complete and precise representation of the attractor. Such refinements may reveal subtle features and complex dynamics that are not captured by conventional FFT analysis, thereby deepening our understanding of the system's behavior.
- Fractal Dimension and Local Dynamics: Since the parabolic shape is observed within a specific frequency range, it may be worthwhile to explore the fractal dimension or local dynamics within this interval. Calculating measures like the correlation dimension or the local Lyapunov exponent in this region may offer insights into the underlying functional form and enhance our understanding of the system's chaotic nature."

Conflict of interest: The authors declare no conflict of interest.

References

1. Ali-Pacha A, Hadj-Said N, M'Hamed A, et al. Lorenz's attractor applied to the stream cipher (Ali-Pacha generator). Chaos, Solitons & Fractals. 2007; 33(5): 1762–1766. doi: 10.1016/j.chaos.2006.03.009
2. Almutairi N, Saber S. Existence of chaos and the approximate solution of the Lorenz–Lü–Chen system with the Caputo fractional operator. AIP Advances. 2024; 14(1). doi: 10.1063/5.0185906
3. Gleick J. Chaos: Making a New Science. Albin Michel; 1989.
4. Lorenz E. Deterministic nonperiodic flow. J. Atmos. Sci. 1963;20(2).
5. Strogatz SH. Nonlinear Dynamics and Chaos: With Applications to Physics, Biology, Chemistry, and Engineering. Perseus Publishing; 1994.
6. Ali pacha A, Hadj-said N, Belmeki B, et al. Chaotic behavior for the secrete key of cryptographic system. Chaos, Solitons & Fractals. 2005; 23(5): 1549–1552. doi: 10.1016/j.chaos.2004.05.015
7. Ali-Pacha H, Hadj-Said N, Ali-Pacha A, et al. Numerical methods for differential equations as encryption key. Journal of Interdisciplinary Mathematics. 2022; 25(8): 2209–2237. doi: 10.1080/09720502.2021.1947598
8. Asadi A. The Python Book: The Ultimate Guide to Coding with Python. Imagine Publishing; 2015. p. 180.
9. Duhamel P, Vetterli M. Fast Fourier Transforms: A Tutorial Review and a State of the Art. Signal Processing. 1990; 19: 259–299.
10. Schatzman JC. Accuracy of the Discrete Fourier Transform and the Fast Fourier Transform. SIAM Journal on Scientific Computing. 1996; 17(5): 1150–1166.
11. Brigham EO. The Fast Fourier Transform. Prentice-Hall, Englewood Cliffs, NJ; 1974. pp. 80–111.